INTERPOLATING AND EXTRAPOLATING CONTAMINANT CONCENTRATIONS FROM MONITORING WELLS TO MODEL GRIDS FOR FATE-AND-TRANSPORT CALCULATIONS

D.B. Ward and P. Clement
Jacobs Engineering Group, 133 Central Park Square, Los Alamos, NM 87544

K. Bostick
Jacobs Engineering Group, 125 Broadway, Oak Ridge, TN 37830

ABSTRACT

Geostatistical interpolation of groundwater characterization data to visualize contaminant distributions in three dimensions is often hindered by the sparse distribution of samples relative to the size of the plume and scale of heterogeneities. Typically, placement of expensive monitoring wells is guided by the conceptualized plume rather than geostatistical considerations, focusing on contaminated areas rather than thoroughly gridding the plume boundary. The resulting data sets require careful analysis in order to produce plausible plume shells. A purely geostatistical approach is usually impractical; kriging parameters based on the observed data structure can extrapolate contamination far beyond the demonstrated extent of the plume. When more appropriate kriging parameters are selected, holes often occur in the interpolated distribution because realistic kriging ranges may not bridge large gaps between data points. Such artifacts obscure the probable location of the plume boundary and distort the contaminant distribution, obstructing quantitative modeling of remedial strategies.

Two methods of constraining kriging can successfully eliminate these geostatistical artifacts. Laterally, the plume boundary may be controlled using a manually constructed mask that delineates the plan-view extent of the plume. After kriging, the mask is used to set all grid cells outside of the plume to a concentration of zero. Use of non-zero control points is a more refined but laborious approach that also bridges data gaps within the body of a plume and permits use of tighter kriging parameters. These can be obtained by manual linear interpolation between measured samples, or derived from historical data migrated along flow paths while accounting for all attenuative processes. Masking and use of non-zero control points result in a plume shell that reflects the intuition and professional judgment of the hydrologist, and can be interpolated automatically to any desired grid, providing initial conditions for fate-and-transport simulations.

Error maps are a valuable aid in assessing data density, identifying areas that require additional sampling, or that must be filled by control points, if additional sampling is impractical.

INTRODUCTION

Quantitative analysis of groundwater contamination requires the construction of a realistic three-dimensional plume shell, mapped to the grid used for fate-and-transport simulations (e.g., MODFLOW/MT3D). Because hundreds of thousands of cells may be involved, manual contouring is impractical. Among many interpolation algorithms available, geostatistics (i.e., kriging) is the most powerful and flexible. Even so, it cannot be blindly applied, especially for the statistically limited data sets typically available for groundwater contamination.

The distribution of monitor wells selected for site characterization typically does not lend itself to geostatistical methods of contouring for determining the nature and extent of contamination. Because wells are expensive, cost minimization dictates that they should be sited based on knowledge of source areas, flow paths, and contaminant behavior. Thus, for a contaminant plume on a large site, there may be numerous wells completed within the body of the plume, useful for refining estimates of mass and locations of hot spots. The margins of the plume may be only roughly delineated by a scattering of wells, and very few wells may exist in areas believed to be lacking contamination. Although the center of mass can be reasonably interpolated by kriging, regulatory agencies and the public may be more concerned about the margins of the plume, the iso-surface along which concentrations drop below the drinking water maximum concentration limit (MCL). A purely geostatistical approach performs poorly in this case because of the sparseness of measurement points. At locations distant from measurement points, kriging returns results that tend toward the mean of the data set, extrapolating significant concentrations into regions that should be contaminant-free. A purely geostatistical analysis often exhibits the following problems:

- Poor representation of the plume boundaries,
- No elongation (the normal "cigar shape") in the direction of groundwater flow, and
- Low confidence where data density is low or irregular.

Although kriging works well for densely gridded sample sets, and can often adequately define the center of mass from typical characterization data, several manual adjustments based on site hydrology and conceptual plume geometry can dramatically improve the plausibility of kriging:

- Restrict the *range* and *search radius* to physically meaningful values,
- Remove extrapolations into areas lacking observations (artifacts) by masking the plan-view extent of the plume,
- Incorporate kriging anisotropy based on knowledge of groundwater flow directions and plausible plume geometry, and
- Add non-zero control points to bridge gaps in the data distribution where the plume is believed to exist.

KRIGING METHODOLOGY

The reader is presumed to have a basic understanding of geostatistics, and is referred to Isaaks and Srivastava (1) or the introductory chapters of Deutsch and Journel (2) for background information. Analyses discussed here used the kriging module in GMS (3), which is an implementation of the GSLIB kriging routines (2). GMS also provides visualization tools for displaying the resulting concentration field and experimental versus model variograms.

Kriging is a three-step process, beginning with processing the field data to tabulate the degree to which pairs of observations are correlated as function of separation distance. Next, geostatistical parameters are selected that mimic the observed correlation as closely as possible. Finally, gridded values are calculated using the field data and model parameters. This paper utilizes ordinary kriging, which adapts to local trends but presumes that the field data show no overall trend across the area of interest. The geostatistical basis for kriging is summarized in the variogram, a plot of variance (the inverse of correlatedness) versus distance (e.g., Figure **1**a), illustrating both the observed relationship obtained from the field data (step 1) and the simulated relationship reflecting the selected model parameters (step 2).

Key parameters controlling the kriging process are presented and described in Table I. This list is not exhaustive, but the unlisted parameters exert only a secondary influence on the final result. The kernel of the geostatistical model is contained in the *nugget*, *contribution*, *range*, and *model function* parameters. In this paper, *nugget* is taken to be zero, a spherical *model function* is always used, and, because ordinary kriging normalizes the weighting factors, the *contribution* serves only as a scaling factor for the model variogram but does not affect the interpolated concentrations.

Table I. Definition of major kriging parameters used in GMS.

Parameter	**Definition**
azimuth (*ang1*)	First rotation of the principal axis. Angle measured clockwise from the *y* axis in the *xy* plane when viewed from above.
dip (*ang2*)	Second rotation of the principal axis. Angle measured down from the horizontal when viewed from the positive principal axis.
plunge (*ang3*)	Third angle of rotation, around the principal axis. Angle measured clockwise when viewed from the positive principal axis.
γ	Variogram *y* axis; a measure of the variance as a function of distance between sample pairs.
distance	The distance separating a pair of samples.
Model Parameters	
nugget	Statistical variance present in adjacent samples, where distance = 0.
contribution (*sill*)	A scaling factor controlling the plateau height of the model variogram. For ordinary kriging, the *contribution* has no effect on the interpolated values because all of the kriging weights are normalized.
range	The distance within which measurements show significantly greater than random correlation.
model function	functional form relating γ to *distance*, e.g., spherical, exponential, Gaussian, etc.
anis1	Transverse anisotropy factor, relative to the principal axis (y axis, unless modified by *azimuth*, *dip* and *plunge* values). Can have any value between 0 and 1.
anis2	Vertical anisotropy factor, relative to the principal axis (y axis, unless modified by *azimuth*, *dip* and *plunge* values). Can have any value between 0 and 1.
Interpolation Parameters	
search radius	The principle radius of the ellipsoid around a grid point to be searched for measured data. Set equal to the *range* model parameter for concentration maps, or set equal to the size of the model for error (variance) maps.
anis1	Horizontal anisotropy factor, set equal to the *anis1* model parameter.
anis2	Vertical anisotropy factor, set equal to the *anis2* model parameter.

( ) = alternate nomenclature (2,1).

For realistic kriging of groundwater contaminant concentrations, the *range* is the most critical parameter. Physically, the *range* can be thought of as the maximum distance at which a field observation provides information. For example, a *range* of 1000 feet (ft) implies that for a given point of interest, observations up to 1000 ft distant tell something about the concentration at that point. The actual weight given to an observation depends on the *model function* as well, with closer observations receiving greater weight. The *range* can be anisotropic to reflect groundwater flow patterns, with the direction anisotropy controlled by the *azimuth*, *dip*, and *plunge*, and its magnitude specified by *anis1* and *anis2*.

The *search radius* is an important modifier for the *range*. For groundwater characterization, in which monitor wells are not placed on a grid, but rather are sited to delineate the magnitude and extent of contamination, the *search radius* should be same as the *range*. This way, in areas outside the *range* of any observations, there will be nothing to krige so concentrations of zero will be recorded. In contrast, the default *search radius* in GMS is equal to the maximum dimension of the area to be kriged. In this case, observations at distances greater than the *range* all receive low but equal weights, so areas outside the *range* of any observations will have concentrations close to the average of all observations. For groundwater contamination, this is clearly at odds with the plume geometry as revealed by the field data.

ANISOTROPY AS A CRITICAL KRIGING PARAMETER

Generally, contaminant plumes are advected from relatively small source areas by flowing groundwater, resulting in a classical "cigar" shape as contamination moves along flow lines and is spread longitudinally, transversely, and vertically by dispersive processes. Because of this elongation in the direction of groundwater flow, the effective *range* is large parallel to groundwater flow and progressively smaller in the transverse and vertical directions. Consider an observation from the core of a large plume several thousand feet long, a few hundred feet wide, and perhaps one hundred feet thick. From the general outline of the plume, one would expect that this observation provides information about concentrations for hundreds feet up and downgradient, but at most only a few tens of feet vertically, with transverse somewhere in between. Ideally, it should be possible to relate plume spreading to hydraulic dispersivities used in solute transport modeling, but real plumes confound this approach because of meso- and macro-scale heterogeneity in the aquifer. Also, plume modeling is typically a precursor to transport modeling, rather than being an iterative process, because of time and budget constraints.

In practice, the *range* and its associated directions and anisotropy are chosen in order to produce a plume shell that is consistent with the conceptual model of the plume. In a perfect world, data coverage would be sufficient to construct directional variograms that would reveal the appropriate longitudinal, transverse, and vertical ranges. Groundwater characterization data seldom if ever reaches the necessary density, so the best that can be achieved is delineation of the longitudinal *range* (e.g., the log semivariograms in Figure **1**). Use of other variograms (e.g., the pair-wise relative semivariogram in Figure **2**) can reveal shorter ranges, but their interpretation is dubious and therefore no less subjective than the qualitative criterion of achieving agreement with the conceptual plume model.

This process of selecting the *range* and associated parameters is illustrated in Figure **1** for two-dimensional data, but is equally applicable in three dimensions. This two-dimensional data set was created from three-dimensional monitoring data by using the maximum detected contaminant concentration at each xy location. Figure **1**a shows the variogram and results of kriging assuming an isotropic *range* of 2000 ft. This *range* is supported by the variogram and is realistic for the long axis of the plume, aligned with the overall north-to-south groundwater flow in this area. Transversely, however, this *range* produces arcs of contamination extrapolated into areas of no data and no expected contaminant. Similar effects occur in three dimensions with an isotropic *range*. Because of such artifacts, the resulting estimates of contaminated area and volume and contaminant mass can be too large by an order of magnitude.

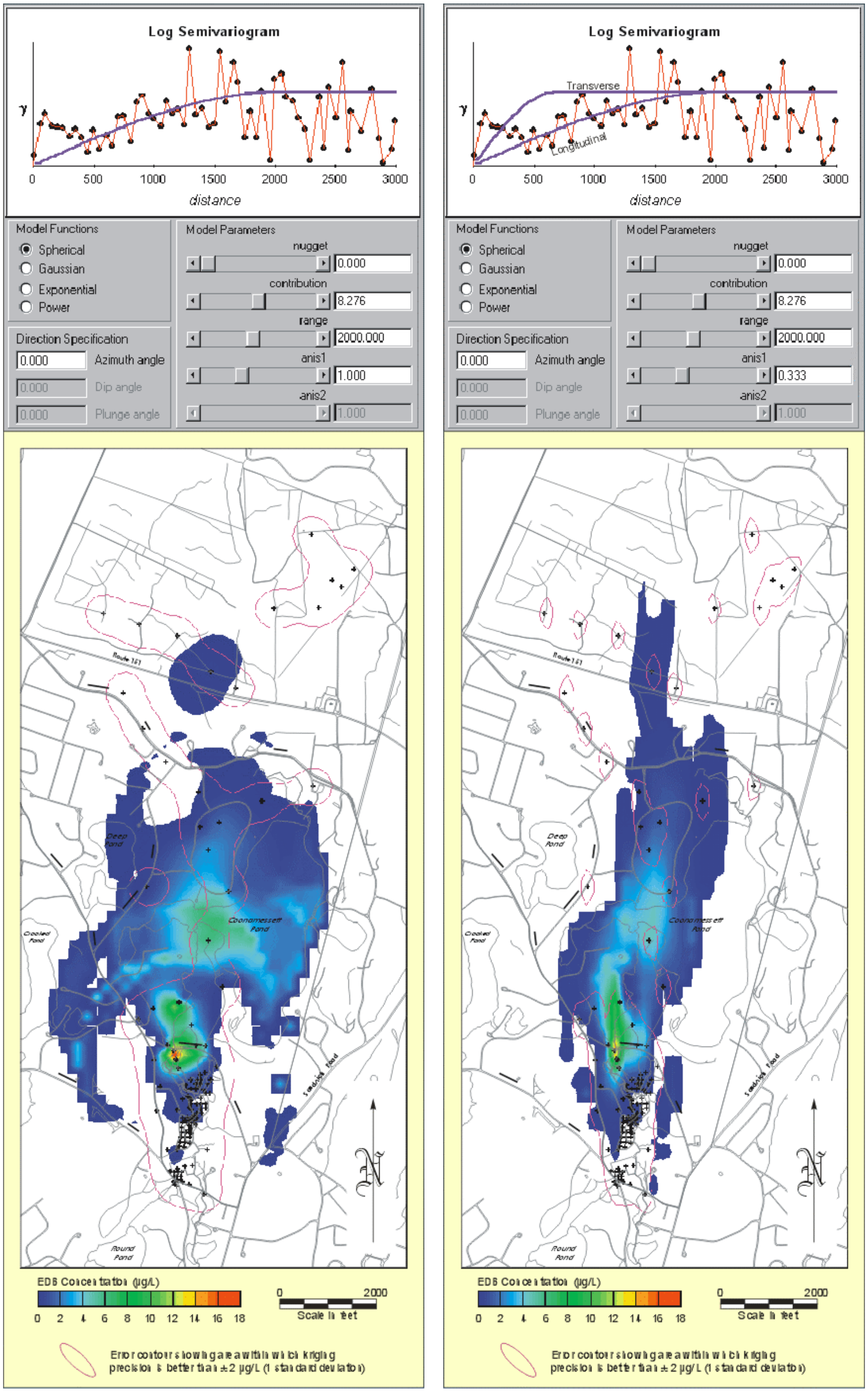

(a) (b)

Fig. 1. Two-dimensional variograms and kriging with isotropic parameters (a) and transverse anisotropy of 0.333 (b).

For the same data set as in Figure **1**a, using an anisotropic range produces a much more realistic plan-view plume (Figure **1**b). This was accomplished by setting *anis1* to 0.333 with the principal direction oriented north-south in the horizontal plane, reducing the effective east-west range by a factor of 3 as illustrated by the model variograms. Note that the experimental variogram contains little evidence of the shorter-range transverse correlation. The plume is elongated parallel to groundwater flow (north to south), but still exhibits low-concentration artifacts in areas lacking monitoring data. Such artifacts could be further reduced by using a shorter *range* with the same anisotropy, but the plume begins to break up into discontinuous blobs as the *range* is decreased. This problem is discussed in depth in a later section.

For the same plume, applying this subjective process to determine the appropriate anisotropy for the full three-dimensional data set results in the plume shell portrayed in Figure **2**. The transverse anisotropy (*anis1*) remains 0.333, and the vertical anisotropy was set to 0.07 to produce a realistic vertical distribution. Thus, the effective range in the vertical direction is smaller by a factor of ~14. The measured data were plotted as pairwise relative semi-variograms, with separate results for each principal axis. The pairwise plotting produced the most highly correlated variogram, but even so, the measured data support only the modeled vertical variogram. This highlights the subjectivity inherent in applying geostatistics to limited data sets; the data are insufficient to constrain the kriging parameters, so they must be estimated based on experience and reasonableness of results.

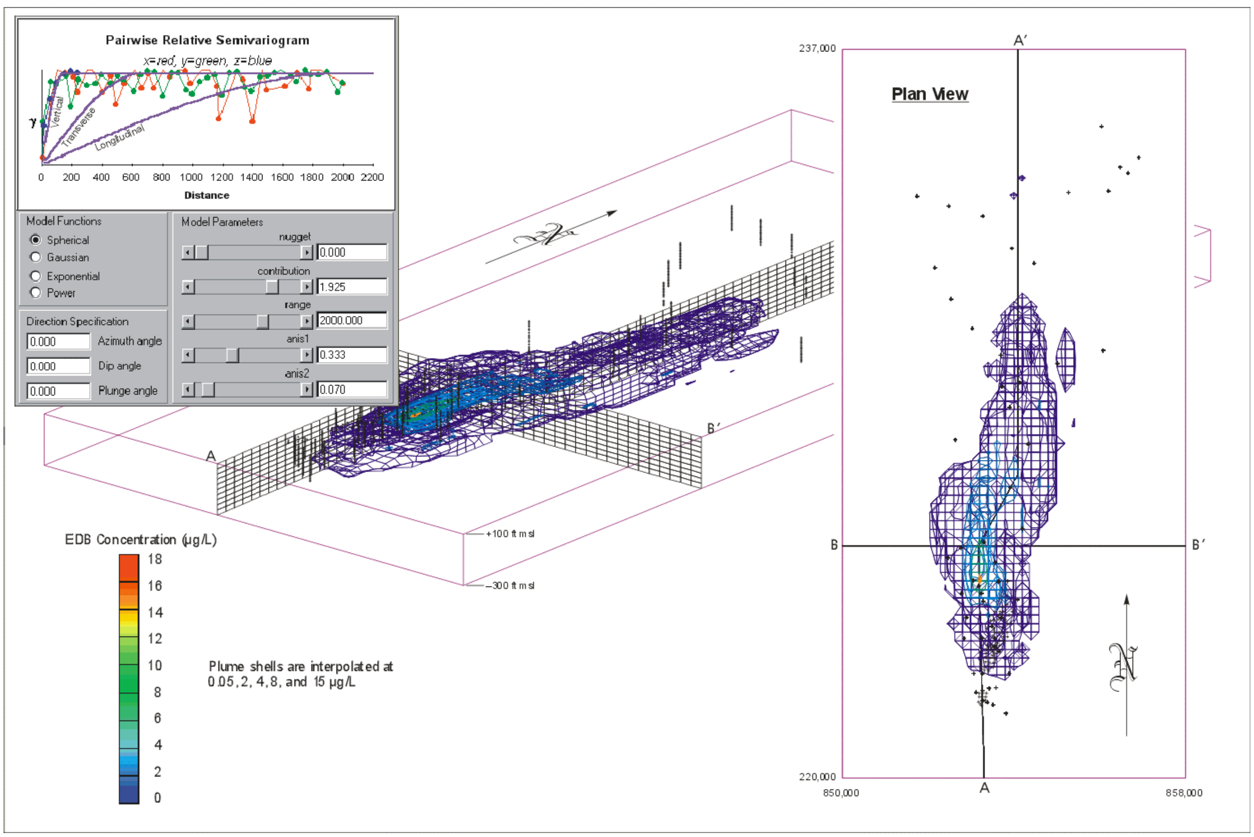

Fig. 2. Three-dimensional kriging using anisotropy.

PLAN-VIEW MASKING FOR ARTIFACTS

In plan view, geostatistical artifacts can be eliminated by masking the lateral extent of the plume. Although such truncation may produce abrupt lateral changes in concentration along the plume boundaries, the plan view will agree with the conceptualized plume and thus be readily understood and accepted by regulators and other stakeholders. When reasonable vertical anisotropy is used, the kriged vertical extent of contamination is typically less of an issue than its lateral extent. In feasibility-study modeling of remediation options, demonstrations of plan-view treatment can provide an adequate basis of comparison for selection of a final remedy. Only in the design stage does it become necessary to take a more critical look at the details of the vertical distribution of contamination.

Figure **3** uses the same anisotropic kriging parameters as Figure **2** to obtain a realistic shape, but is masked at the conceptual lateral extent of contamination (0.004 µg/L in this case) to remove geostatistical artifacts from the plan-view appearance of the plume. Differences in the internal structure of the plume are due to the differing isosurfaces contoured in each figure. Concentrations outside of the mask are set to zero, truncating the plume to a hydrologically plausible outline and eliminating the problem of extrapolation into areas lacking data coverage. The vertical distribution of contamination still exhibits some geostatistical artifacts, with an outlier unconnected to the main body of the plume at an elevation just above 0 ft mean sea level (msl), and with unrealistic structure for the leading edge. At the leading edge, vertical flow is predominant as the plume discharges to surface water, in violation of the assumptions used to establish the average anisotropic kriging parameters for the bulk of the plume.

This could be remedied by using separate kriging parameters for the leading edge, extending the idea of masking to permit kriging with multiple parameter sets. In this case, each subregion of a plume, in which groundwater flow directions are nearly uniform, would be kriged and masked separately, and then the resulting grid arrays would be added to create a composite plume shell.

The masking technique is rapid to implement in GMS, requiring comparatively little manual input. A polygon of the plume outline, created using the map module, is used to initialize a three-dimensional array for the kriging grid with values of 1 within the plan view of the plume, and values of zero elsewhere. The product of the mask array and the concentration array, obtained using the GMS array calculator, contains the desired result, i.e., concentrations forced to zero outside the mask outline.

CONTROL POINTS FOR ARTIFACTS AND GAPS

Synthetic data (control points) can be added to the set of observed data to constrain geostatistical extrapolation outside the known extent of contamination, and to bridge gaps between widely spaced monitoring wells within the plume. Whereas masking is an after-the-fact brute-force approach, control points modify the input data set and permit fine-tuning of the kriging process itself. The need for control arises because the observed data are inadequate to provide geostatistical definition of kriging parameters. Instead, the kriging parameters become another set of knobs to twist in an effort to produce a three-dimensional distribution of contamination that agrees with the conceptual model of the plume. The values assigned to control points are also guided by the conceptual model; control points used to bound the plume have zero concentration, whereas linear interpolation using nearby observations is useful for gap-bridging control points within the plume. Kriging used in this manner is no longer a quantitative tool requiring a massive data set, but has become a practical visualization tool capable of providing realistic depictions of both the center of mass and extent of contamination that can be presented to regulatory agencies and the public with little additional explanation. After all stakeholders are in consensus with the

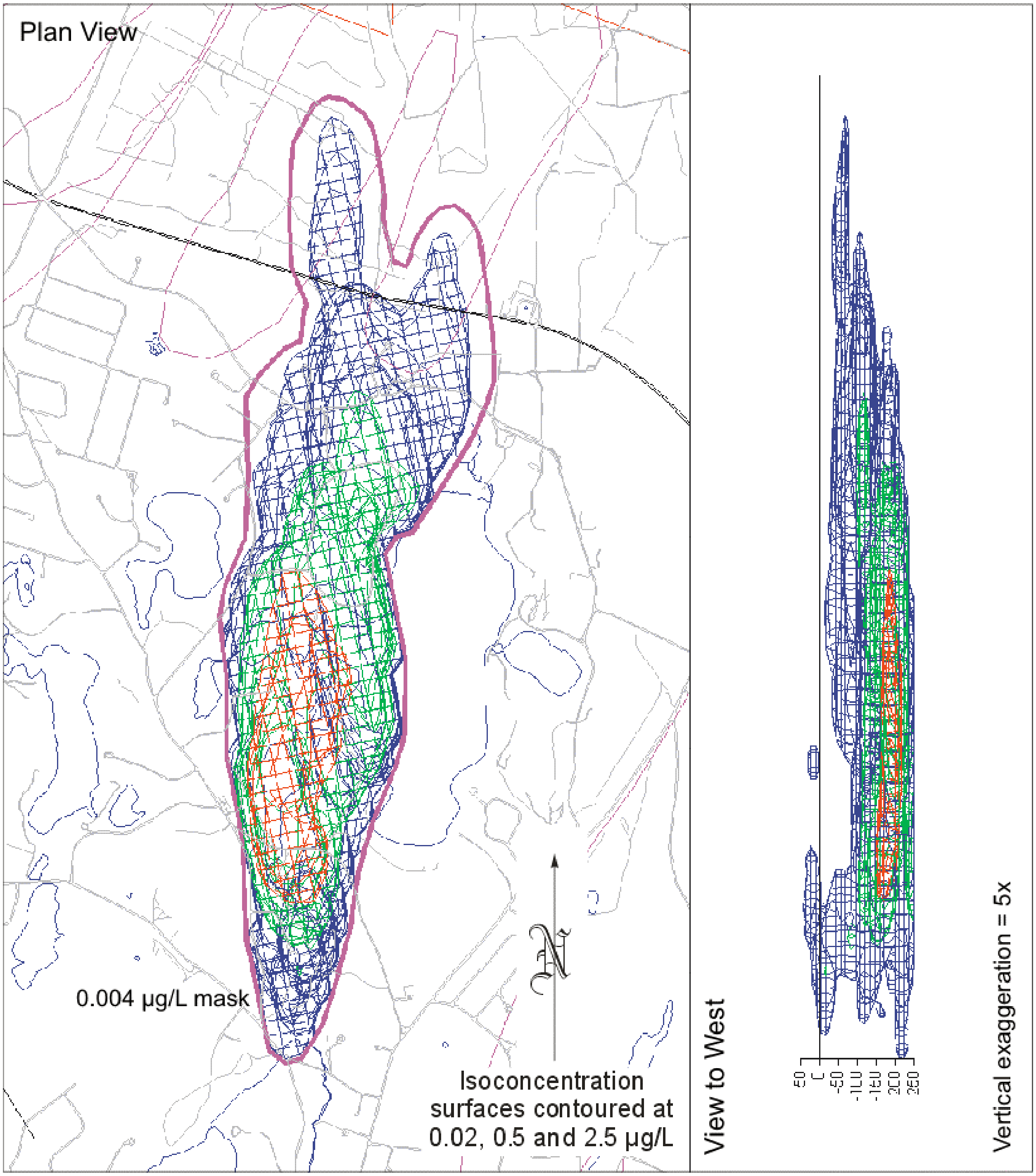

Fig. 3. Three-dimensional kriging using a plan-view mask.

plume geometry, the plume can be kriged onto any desired grid to provide initial concentrations for contaminant transport modeling.

Constraining geostatistical extrapolation by adding bounding control points with concentrations of zero would seem to be a straight-forward proposition, but in practice often yields surprising results, particularly with three-dimensional data sets. Consider the case discussed above for masking (Figure **3**), in which the leading edge of the plume becomes quite narrow as flow lines converge to a discharge zone. Here, kriging parameters were adjusted to provide a realistic depiction of the core of the plume. In the absence of the mask (Figure **2**), the margins of the plume's leading edge are much too broad because of the abundance of observations there combined with the comparatively large kriging *range* of 2000 ft. Adding "walls" of bounding control points around the leading edge had only a small effect on the extent of contamination as denoted by the 5 μg/L isosurface (the MCL here). The "walls" were two-dimensional arrays with horizontal spacings of 100 ft and vertical spacings of 10 ft. Although there were hundreds of bounding control points, their interaction with the observed data was unable to blank out the contribution of high-concentration observations in the core of the plume.

The seeming failure of bounding control points to constrain kriging is attributable to the large *range* used in that example, which extended the influence of high-concentration observations to unreasonable distances in certain directions, but was required in order to produce a plausible geometry for the plume core. When the *range* is reduced substantially, the need for bounding control points is similarly reduced, and they become much more effective where they are needed. Under this philosophy, the *range* and anisotropy parameters can be selected for physical plausibility rather then being dictated by the density of observations and the need to tie the observations together into a coherent plume. For example, the large *range* used in Figure **2** is at odds with the conceptual model of the plume, and results in a radius of influence around each observation of 2000 ft parallel to groundwater flow, 667 ft transverse, and 140 ft vertically. A more realistic *range* of 560 ft, smaller by about a factor of four, is illustrated in Figure **4** for another plume in the same geologic setting. The resulting radius of influence is 560 ft parallel, 190 ft transverse, and 15.7 ft vertically. Although the true correlation distance is probably less by another factor of two to four, this is a substantial improvement.

Because of the wide spacing of the observed data, using a smaller *range* often causes plumes to break apart, as illustrated in Figure **4**a. This example, lacking control points, shows two main zones of contamination separated by an interval lacking observations. Because the two zones lie along the same groundwater flow trajectory, it is reasonable to assume that the intervening aquifer is also contaminated. A second less conspicuous problem is related to the averaging nature of the kriging algorithm: a single point with no others within its radius of influence will not be kriged no matter what its concentration (assuming that the *search radius* has been set equal to the *range*). A smaller *range* can thus result in a substantial number of orphaned non-zero observations.

Non-zero control points added judiciously to the data set can fill data gaps and link outlying observations to the main body of the plume, as shown in Figure **4**b. In this example, the set of observations consists of 178 values, which have been combined with 71 non-zero control points and 66 bounding control points. Concentrations for non-zero control points were estimated manually by linear interpolation from nearby observations. The final set of control points was arrived at by labor-intensive trial and error to constrain the plume to a hydrologically plausible shape. The final plume shell reproduces the classic cigar-shape in plan view, with concentric zones of progressively higher concentration toward the core. The two high-concentration zones evident in cross-section may have originated from closely spaced but distinct sources, and the unconnected zone of low concentration ahead of the main body may be the result of ongoing remediation efforts. This plume shell both honors the field observations (within the constrains imposed by the averaging tendencies of kriging), and is plausible based on knowledge of site hydrogeology and source-area history.

For this plume, variograms with and without control points indicate only a very short *range*, which appears to coincide with the vertical radius of influence. Adding control points has smoothed much of the variation at greater distances, but has not altered the underlying trend. The dominance of vertical relationships in these non-directional variograms arises from the closely spaced (vertically) borehole data

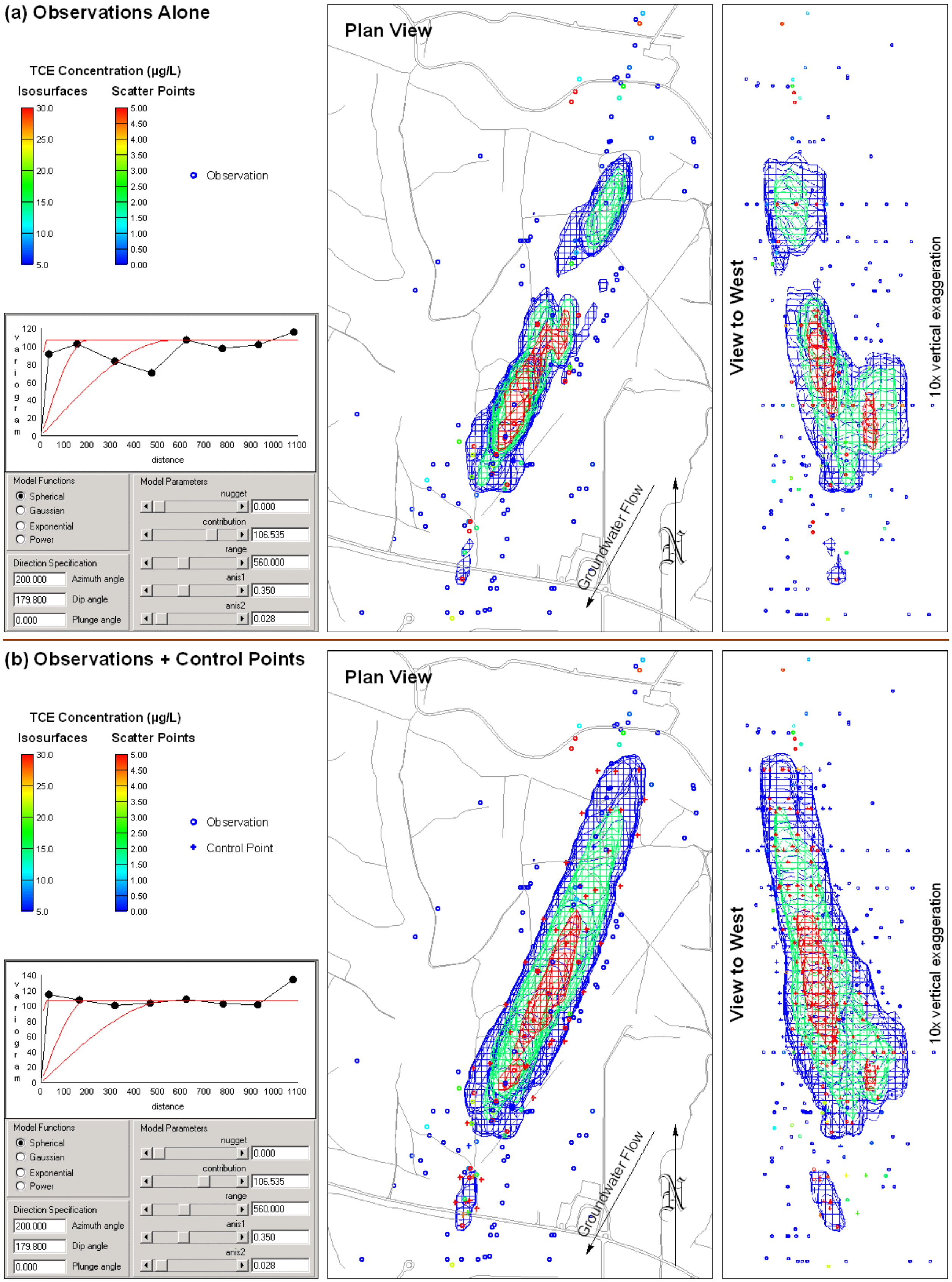

Fig. 4. Three-dimensional kriging of field data only (a) and with control points (b).

that has been combined with data from monitoring wells to create the observed data set. During drilling, borehole water samples were collected approximately every ten feet, giving a detailed vertical profile at a single location. In contrast, monitoring wells are typically spaced several hundred feet apart. Because concentrations often change dramatically from sample to sample in a given borehole, the vertical signal is by far the strongest at short distances in the variograms. In some cases, directional variograms may reveal other trends, but such detailed analysis is not merited given the qualitative nature of the kriging approach presented here.

ERROR MAPPING TO ASSESS DATA DENSITY

Error mapping provides one means of assessing whether the sampling density is sufficient to define the plume and to identify areas in which further sampling is needed, or control points may be necessary. In addition to kriging concentrations, GMS can map the variance. The standard deviation of the interpolation is found by taking the square root of the variance, and provides an easily understood measure of the error associated with the kriging process at each grid point. Kriging parameters for error mapping are the same as for concentration mapping, with the exception of the *search radius*. For error mapping, the *search radius* should be set to the length of the diagonal of the kriging grid. This way, in areas of no samples, the standard deviation will tend toward a maximal value, the standard deviation of the entire data set. In areas of high data coverage, the nearest observations should have roughly similar values, resulting in lower standard deviations. Exceptions to this may occur, however, in areas of extreme small-scale heterogeneity, resulting in high standard deviations even in densely sampled areas. This is sometimes seen in the core of complex plumes, and is an indication that the true geostatistical *range* is much less than the selected kriging *range*.

In Figure **5**, these two drawings show standard deviations for the two-dimensional plume in Figure **1** for the isotropic case and with a transverse anisotropy of 0.333. In these examples, the northern portion of the plume (trailing edge) is represented by only a few sampling locations, and is largely unbounded geostatistically. Interpretation of plume geometry in these areas must rely knowledge of site hydrology, geochemistry, and source history. The southern portion of the plume (leading edge) has been densely sampled, past the point of diminishing returns for the purpose of plume characterization. The cluster of sampling points here did little to enhance statistical certainty; fewer points would have been adequate.

SUMMARY

Kriging is a useful tool when combined with knowledge of site hydrology, history, and mechanisms affecting contaminant fate and transport. If kriging is applied blindly, ignoring these factors and without compensating for deficits in the observed data, the results will be specious. To obtain plausible and realistic results, it must be recognized that the limited data sets typically obtained from site characterization preclude a rigorous geostatistical approach; kriging parameters must be manually adjusted to obtain results that are reasonable. One of the most important manual adjustments is to align the principle kriging axis with the direction of groundwater flow. This permits realistic assignment of geostatistical anisotropy to account for longitudinal elongation and vertical restriction of the plume.

Geostatistical artifacts unsupported by observations often remain when the kriging *range* is large enough to produce a coherent plume. Although such kriging often produces a realistic representation of the core of the plume and may be suitable for simulating pump and treat systems that extract from the center of mass, the extent of contamination may be significantly exaggerated. Such artifacts can be excised manually by masking the plume to its conceptual boundary. Masking is also useful for large plumes with

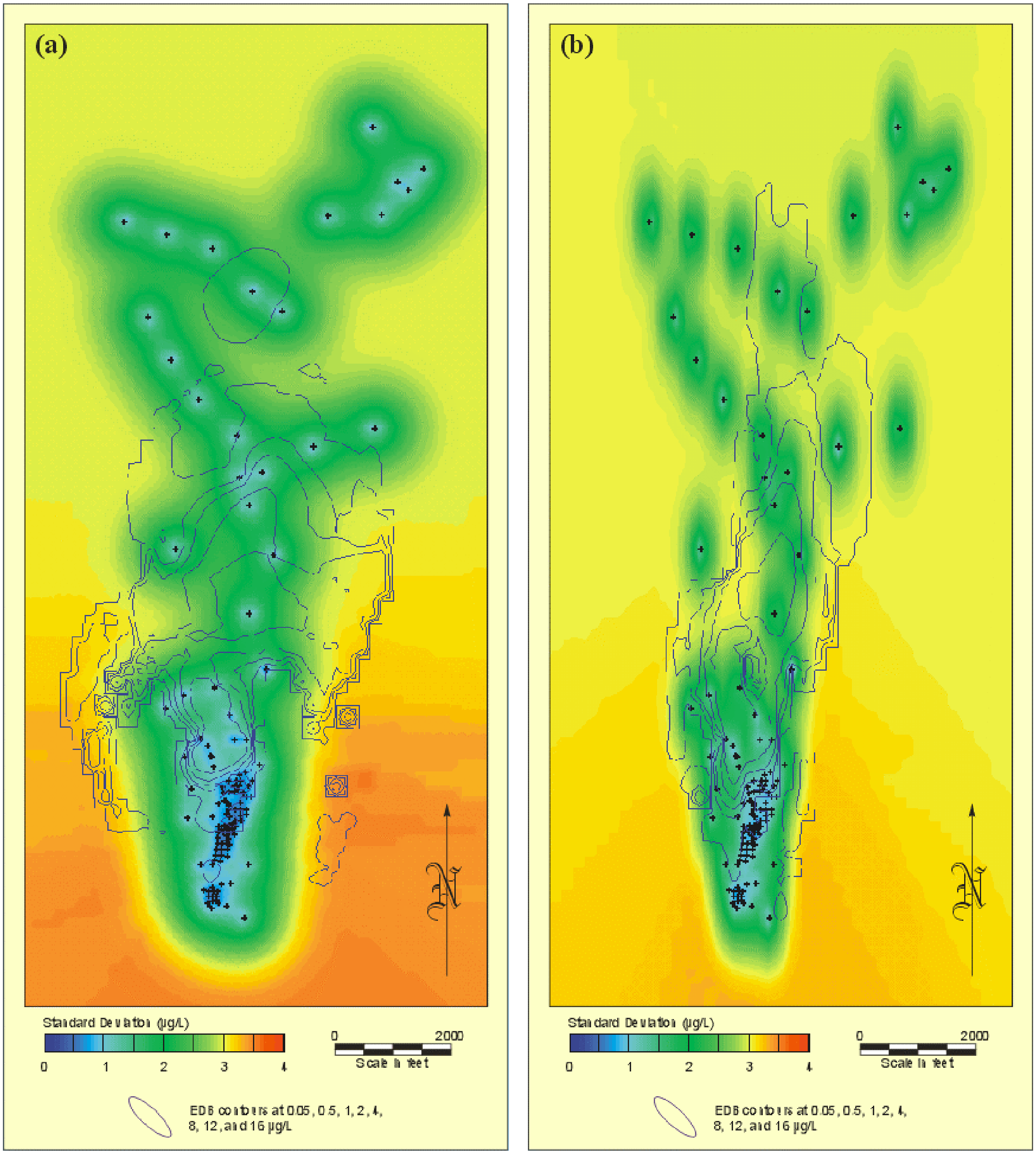

Fig. 5. Standard deviation of two-dimensional kriging with isotropic parameters (a) and transverse anisotropy of 0.333 (b).

varying directions of groundwater flow. In this case, each subregion is kriged with its own parameters, and then all subregions are combined to create the total plume.

Fine-tuning of the kriging process is possible through the use of control points. Non-zero control points are essential for producing a coherent plume when the kriging *range* is reduced physically realistic values. These control points are needed to fill the gaps between the more widely spaced observations. Addition of such control points is time-consuming and requires trial-and-error to constrain the plume to a hydrologically plausible shape. The effort is justified where risk or points of compliance are of concern, or if the remedial goal is complete plume capture.

Error maps can be a valuable aid in the design of a sampling program that minimizes the number of sampling locations (and therefore cost) while ensuring adequate data density. Such maps also highlight data gaps that must be filled by control points, if additional sampling is impractical.

REFERENCES

1. E.H. ISAAKS and R.M. SRIVASTAVA, *An Introduction to Applied Geostatistics*, Oxford University Press, New York (1989).
2. C.V. DEUTSCH and A.G. JOURNEL, *GSLIB: Geostatistical Software Library and User's Guide, Second Edition*, Oxford University Press, New York (1998).
3. Dept. of Defense Groundwater Modeling System (GMS) version 2.1, Brigham Young University, Provo, Utah (1998).